Modeling and Instrumentation for Fault Detection and Isolation of a Cooling System

Philippus J. Feenstra[1], Eric-J. Manders[2], Pieter J. Mosterman[3], Gautam Biswas[2] and Robert J. Barnett[4]
[1]Department of Electrical Engineering, Twente University
P.O. Box 217, 7500 AE Enschede, The Netherlands
p.j.feenstra@student.utwente.nl
[2]Department of Electrical Engineering and Computer Science, Vanderbilt University
P.O. Box 1824 Station B, Nashville, Tennessee 37235
{manders,biswas}@vuse.vanderbilt.edu
[3]Institute of Robotics and Mechatronics, DLR Oberpfaffenhofen
P.O. Box 1116, D-82230 Wessling, Germany
Pieter.J.Mosterman@dlr.de
[4]Department of Mechanical Engineering, Vanderbilt University
joelbar@vuse.vanderbilt.edu

Abstract

Functional redundancy techniques for fault detection and isolation (FDI) in dynamic systems requires close interaction between system instrumentation, modeling and analysis. Effective FDI requires detailed and accurate models to track and analyze system behavior, including transient phenomena that result from faults. It also requires appropriate instrumentation technology to provide the measurements to capture and analyze system behavior. Models and measurements must be matched carefully to provide sufficient observability and effective analysis. In this paper we demonstrate the development of FDI systems for complex applications by presenting the modeling and instrumentation of an automobile combustion engine cooling system. We have developed a qualitative parameter estimation methodology for FDI. A system model is represented as a graph that captures the dynamic behavior of the system. To demonstrate the applicability a small leak is artificially introduced in the cooling system and accurately detected and isolated.

1 Introduction

In complex industrial processes, operational safety and reduced down-time are ensured by hardware redundancy and localized hardware safety mechanisms (e.g., check valves). To reduce cost, hardware redundancy is increasingly being replaced by use of functional redundancy techniques which relies on a *model* of the system under scrutiny and uses functional relations between system variables to infer discrepancies between measured variables. When such discrepancies occur, a fault is detected and appropriate action has to be taken. Fault detection followed by a fault isolation stage to accurately locate the failing physical component, establishing the fault detection and isolation (FDI) paradigm.

Fault detection and isolation in complex dynamic systems requires the use of modeling approaches that capture system dynamics and the transients that arise when faults occur. In previous work [11], we have developed a systematic approach using bond graph modeling to derive the *temporal causal graph* (TCG) representing the functional relations of a system subject to FDI. The inherent physical constraints of a bond graph model (conservation of energy, conservation of the physical state, continuity of power) result in well constrained models that prevent the generation of spurious results, one of the most important drawbacks of traditional qualitative methods used in artificial intelligence approaches to the diagnosis problem. The genericity of the bond graph modeling approach allows seamless integration of multi domain models (e.g., electrical,

0-7803-6312-4/00/$10.00 ©2000 IEEE.

mechanical, hydraulic) into one representation.

Another critical issue in FDI is the instrumentation of the system. The FDI quality is typically constrained by the measurements that are available and their quality. The bandwidth of the measurement system determines the range of values of the modeled time constants. A larger bandwidth allows the inclusion of smaller time constants, and, therefore, functional redundancy is enhanced. Furthermore, even in a qualitative framework, more precise sensors allow for a smaller error tolerance (typically between 2% and 5% of the nominal value), and, therefore, deviating values may be detected that otherwise go unnoticed. In our qualitative FDI approach, implemented as the TRANSCEND system, measured deviations drive the isolation process, therefore, the ability to identify and characterize deviations is the key to diagnostic analysis. We demonstrate that this implies a tight coupling between the instrumentation and the model of a system, which requires an integrated approach to achieve effective FDI.

In this paper we show how the qualitative approach to FDI, embodied by the TRANSCEND system applies to the fault isolation in an automobile engine cooling system test bed. To this end, a bond graph model of the system is designed that includes mechanical, thermal, and hydraulic phenomena. The model is automatically converted into a TCG representation that serves as the input to TRANSCEND. The model of the cooling system is described in Section 2 where the challenge is to capture the level of physical detail corresponding to the bandwidth of the measurement system and relevant to the set of faults we need to diagnose. Section 3 describes the experimental setup. Section 4 describes the FDI approach and presents and interprets the results. Section 5 summarizes the conclusions from this work.

2 Modeling

Modeling for diagnosis requires the construction of a parsimonious model that captures all phenomena that are important to distinguishing the different faults in the system However, the model must not include phenomena that cannot be observed with the available instrumentation. To isolate faults accurately, the system needs to model nominal behavior as well as transients that occur after a fault manifests. This requires that the model captures the system dynamics quite precisely, even in the presence of faults.

2.1 The System

An automotive cooling system uses a liquid coolant pumped through passageway in the engine block by a centrifugal pump driven by the crank axis. Figure 1 shows a block diagram of the fluid path. Starting at the pump, coolant is pumped into the lower part of the engine block. The coolant passes through the block and through passageway in the cylinder, and heads up to the intake manifold from where it flows back towards the front of the engine. A thermostat regulates the flow of coolant at this point. Before the engine reaches its desired temperature the thermostat is closed and the coolant is pumped back into the engine block without passing through the radiator. When the engine reaches its desired temperature, the thermostat opens and the coolant now circulates through a hose to the radiator. The radiator acts as a heat exchanger and air blown through the radiator by a fan and/or motion of the vehicle cools the coolant. Controlling the flow of coolant in this manner ensures that the engine reaches normal operating temperature as quickly as possible.

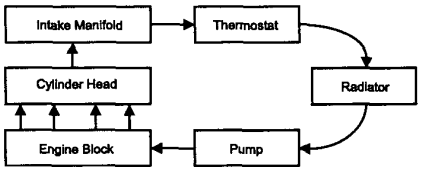

Figure 1. A block diagram of the engine cooling system.

2.2 Model

We derive the cooling system bond graph model in three stages that correspond to constructing partial models in the mechanical, hydraulic, and thermal domains. Figure 2 shows the complete model of the cooling system. Energy exchange between the mechanical and the hydraulic domain occurs in the pump through rotation of the crank axis to produce coolant flow. It is indicated by the power coupling of bond 51. The interaction between the mechanical and the thermal domain is negligible. Measurements indicate that the *power* interaction between the hydraulic and thermal domains is negligible because the coolant is basically incompressible. However, there is a *convective* connection between the hydraulic and the thermal domain, modeled by signal lines (dashed gray), which will be explained in the discussion of the thermal part. There

is no influence *from* the thermal domain to either the hydraulic or the mechanical domain.

To enable easy construction of the thermal part, this part is modeled using pseudo bond graphs. Since the fluid is assumed to be incompressible, the fluid part can be modeled either using pressure and mass flow rate as conjugate pairs (pseudo bond graphs) [5] or pressure and volume flow rate as conjugate pairs (true bond graphs). To establish direct links between the mechanical and fluid systems they are both modeled as true bond graphs. As a result the convection resistors that model convective heat flow in the thermal domain are controlled by the volume flow rate.

2.2.1 The Mechanical Domain

The engine crank axis is modeled by a flow source. The transmission ratio between the crank axis and the pump, due to the connecting V-belt, is represented by a transformer where the efficiency attributed to the pump losses is modeled by the resistor R_{effic}. The inertia of the pump rotor is taken into account by the inertia I_{pr}. The model of a centrifugal pump can be derived using conservation of power and momentum. This generates by approximation the constituent relations for the torque and the pressure $\tau = K\dot{V}\omega$ and $p = K\omega^2$, respectively [9]. Here $\dot{V}$ is the volume rate, ω the angular frequency and K a constant that depends on the construction of the pump. These relations can be described with a modulated gyrator (MGY).

2.2.2 The Hydraulic Domain

The coolant flows through the engine block to the radiator and back via upper and lower hoses. C_{blair} represents air and steam in the block that embodies compression effects. The thermostat presents a narrow opening and is modeled by resistance and inertial parameters, R_s and I_s, respectively. The fluid path that exists when the thermostat is closed (the primary circuit), is neglected in steady state. The air present at the top of the radiator is modeled by C_{rair}. The flow through the radiator is governed by the parameters R_{rad} and I_{rad}. Two resistances, R_{rluh} and R_{lklh}, are explicitly added to model leakages in the upper and lower hose, respectively. A fault implies their values drop considerably allowing flow out of the system through these elements.

2.2.3 The Thermal Domain

Two approaches to describe convective heat flow are used in thermodynamics. The Lagrangian approach tracks a fixed packet of particles [5]. The Eulerian approach applies observations made at a fixed point in space through which fluid passes and is more useful in practice [14]. Because of the fixed reference used in the Eulerian description, convective terms will appear in the momentum and energy equations that are not easy to model with true bond graphs. Therefore, *pseudo bond graphs* are used for the modeling of the dynamics. In these models, the connections between bond graph elements and their causality assignment is analogous to bond graphs. However, instead of using entropy flow as the flow variable, the enthalpy flow is chosen. With temperature as the effort variable, the product of effort and flow does not equal power. Though this requires special care when using transformers and gyrators, this drawback is outweighed by the modeling advantage this approach offers.

In pseudo bond graphs, the energy entering a moving fluid, enthalpy h, will split up into two parts (i) the energy carried by pressure and volume and (ii) the convected internal energy.[1] Using the notation of extensive variables, $h \equiv u + pv$, where h is the enthalpy, u is the internal energy, p is the pressure, and v is the volume.

The *convection resistor* [5] is developed in this framework. The energy transport of a moving mass can be viewed as the transport of mechanical, hydraulic, or electrical energy by moving accumulators, like stressed springs, fluid containers under pressure or charged electric capacitors [14]. The convective energy flow from one energy storage element to another is not only a function of the effort flow relation but also a function of the volume flow, these flows are indicated as dashed gray vertices in Figure 2. The convection resistor can be interpreted as a modulated resistor [2] shown in Figure 3 along with its constitutive equations (see also [5]) where $\dot{m}$ is the mass flow, c_p is the specific heat at constant pressure, $\dot{V}$ the volume flow, and ρ is the density of the coolant.

A model of the thermal part is then developed as follows. Energy added to the coolant is modeled by the entropy source, S_f, that represents the combustion process (see Figure 2). This energy is buffered in the block represented by C_{bl} or convected via the upper hose to the radiator. C_u takes the heat capacity of the upper hose into account. The heat capacity of the radiator is C_r. The ambient temperature of the outside air is modeled by the effort source T_{amb}. The convection from the copper to the air is a function of the air velocity (the fan) and is modeled by the modulated resistor R_{ca}. The fan is also driven, just like the pump,

[1] When the flow velocity is relatively high the kinetic energy has to be added.

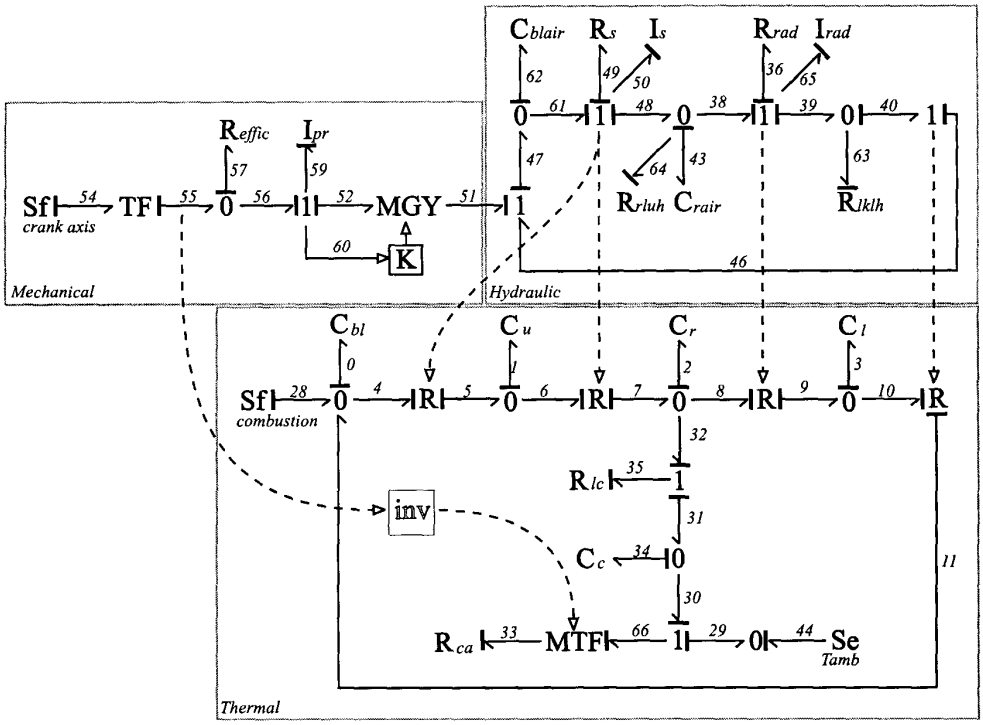

Figure 2. Complete model of the engine cooling system with relations across domains.

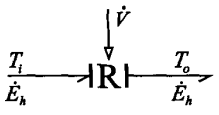

$$\dot{E}_h = \dot{m} c_p T_i = \dot{V} \rho c_p T_i \qquad ; \dot{m}, \dot{V} \geq 0$$
$$\dot{E}_h = \dot{m} c_p T_o = \dot{V} \rho c_p T_o \qquad ; \dot{m}, \dot{V} < 0$$

Figure 3. Convection represented by a modulated two port R and corresponding constitutive equations.

by the V-belt. The exact function between the crank axis angular velocity and the resistance R_{ca} is not required in a qualitative framework. C_c represents the heat capacity of the radiator metal and R_{lc} the conduction from liquid to metal. The energy that does not leave the coolant is convected back to the block, passing through the lower hose C_l. There are no leakage resistances added to the thermal domain because of the assumptions that the energy leakage, if any, is relatively small. If required for fault modeling, a R_{field} convection resistor and an effort source that serves as entropy sink may be added. The inverse of the angular velocity controls the MTF and consequently the heat resistance from the radiator to the outside air. The coolant volume flows derived from the hydraulic part modulate the convection resistors.

3 Experimental System

The experimental system consists of the engine testbed and the data acquisition system.

3.1 Instrumentation of the Cooling System

Details about the engine test bed and the specific sensors have been reported in [7]. In this paper we mention only the location of the sensors in the cooling system needed to for the mapping of sensor location to variables in the model.

The cooling system is currently outfitted with four sensors. Two temperature sensors, T1 and T2, measure temperatures in the leakage valve and in the thermostat, respectively. Two pressure sensors, P1 and P2, measure the pressures in the lower hose, just before the block, and in the upper hose just after the thermostat, respectively.

3.2 Data acquisition

The instrumentation system for TRANSCEND is based on the proposed IEEE-1451 standard for a smart transducer interface for sensors and actuators. This standard enables the development of Internet enabled measurement and control applications [6].

3.2.1 Hardware

Figure 4 shows the instrumentation system. The sensors are network enabled through the use of two hardware components, A Network Capable Application Processor (NCAP), and a Smart Transducer Interface Module (STIM). The interface between the STIM and the NCAP is defined in an IEEE Standard [4]. In addition, the STIM hosts an electronic data sheet that includes all information normally available on a transducer data sheet as well as the calibration coefficients.

The NCAPs used are Hewlett-Packard embedded Ethernet controllers [3], a complete, network ready interface for connecting a STIM to Ethernet. The STIM used in the current configuration ([1]) has two analog inputs and two analog outputs. Each channel has a full analog signal conditioning ASIC with programmable filters, multiple gain setting, offset control and programmable sample rate. A micro controller contains the analog-to-digital converters for the input channels, and the required peripherals to directly support an IEEE-1451.2 compliant interface.

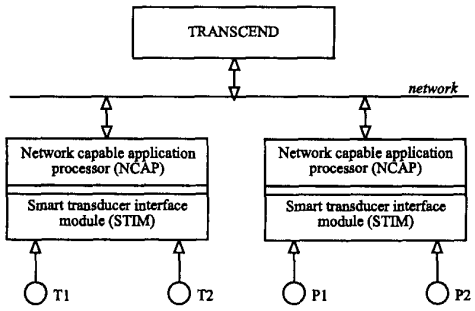

Figure 4. The instrumentation system.

3.2.2 Programming Model

The IEEE 1451 standard defines an information model for measurement and control data (IEEE-1451.1) but an implementation of this standard is not yet available. In the current experiments with the cooling system the data is captured using a different method. The embedded Ethernet controller hosts an embedded web server. An HTTP API provides access to the 1451.2 interface. The communication between an application and the controller then becomes a client-server link. Note that the HTTP API itself is not covered by the standard but specific to the Hewlett-Packard product. The TRANSCEND data acquisition software then consists of a Java application that communicates with the NCAP to obtain sample data by opening a network connection to each NCAP.

The NCAP is configured for a sample time of 1/32(s). The data is processed on-line to derive symbolic input to the diagnosis system [8]. The signal analysis algorithms that extract the symbolic feature data from the raw signals can run on the NCAP itself, in effect pushing the feature extraction step onto the sensor, thereby reducing network traffic.

4 Fault Detection and Isolation

This section gives an overview of the diagnosis approach developed in previous work [9, 11] and presents some results of the cooling system test bed.

4.1 The Diagnosis Approach

Once a bond graph model of the system is designed, a qualitative representation is available that allows temporal reasoning about the dynamic behavior when faults occur. To this end, the causal structure of the system variable relations embodied by the bond graph is made explicit. This results in a temporal causal graph (TCG) that can be used in two stages: (*i*) backward propagation generates a set of possible parameter deviations consistent with a deviating measured variable and (*ii*) forward propagation predicts future behavior of all measured system variables given each of the hypothesized parameter deviations. Details of this methodology are presented elsewhere [9, 11].

Figure 5 shows the TCG of the cooling system that is automatically derived from the bond graph using the HYBRSIM modeling tool [12]. The measurements p_1, p_2, T_1, and T_2 correspond to the edges $e46$, $e62$, $e4$, and $e5$, respectively. If the measured value of p_1 is less than its nominal value, the corresponding model variable in the TCG, $e46$, is marked $-$, $e46^-$. Backward propagation now infers that either $e51^+$ or $e47^-$. Propagation continues until an edge with a parameter relation is traversed, e.g., along the path $e46^- \overset{\pm 1}{\leftarrow} e47^- \overset{=}{\leftarrow} e62^- \overset{\frac{1}{C_{blair}}dt}{\leftarrow} f62$. At this point, the parameter is implicated according to the propagated deviation, i.e., C^+_{blair}, and the upstream variable is marked as well, $f62^-$, to include the case the parameter has not deviated. Backward propagation along

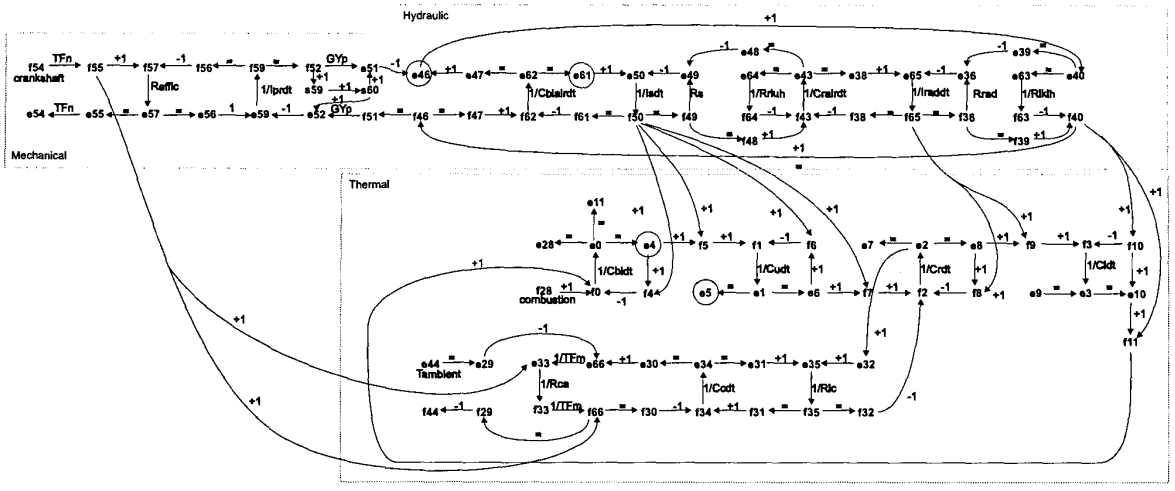

Figure 5. Temporal Causal Graph of the cooling system. Measured variables are indicated as circled vertices

a path terminates when a conflicting assignment to a variable deviation is found

The result of the back propagation is a set of hypothesized parameter deviations consistent with one of the measured deviations. To find the correct parameter deviation, predictions of future behavior are generated by forward propagation and continued monitoring of the predicted behavior. Inconsistency between prediction and measurement causes a parameter deviation to be removed from the set of hypothesized faults.

For the parameter deviation C^{+}_{blair}, forward propagation predicts $e62^{-}$. Further propagation along one path results in $e62^{-} \xrightarrow{=} e61^{-} \xrightarrow{+1} e50^{-} \xrightarrow{\frac{1}{I_s}dt} f50^{\downarrow}$. Note that traversing the temporal relation $\frac{1}{I_s}dt$ (the dt element indicates a time integrating effect) changes the prediction from a 0^{th} order deviation to a 1^{st} order deviation. For this variable, if along other paths no prediction of its 0^{th} order behavior is available, it is considered normal, i.e., $f50^{0,\downarrow}$. Propagation continues until all higher order derivatives of the measured variables are predicted. The maximum order of the prediction is a design consideration and linked to the measurement selection task [13]. When conflicting assignments to the same time derivative arise, this prediction is unknown and further propagated, overwriting any previously assigned predictions of the time derivative. This has an especially disastrous effect in case of algebraic loops, i.e., when there is no delay between two opposing effects. In this case, many variables become unknown which prohibits precise fault isolation.

4.2 Introducing Faults

To test the model for correctness some artificial faults were induced, while the engine was running close to steady state. Here we describe a slow leakage in the lower hose caused by opening a valve.

Figure 6(a) shows the signal data for the lower hose leakage fault ($R_{klh}-$). We can observe that the pressures decrease. The temperatures have a very small slope due to the fact that the temperature had not quite reached steady state when the fault was introduced (i.e., it is no behavioral artifact of the failure) Figure 6(c) shows the FDI results from TRANSCEND. After two time steps the minimum set of fault candidates is obtained. The leak cannot be uniquely isolated because there is not sufficient discriminating information about the system available. For example there is no flow measurement which makes the distinction between R_{rad}, I_{rad} and R_{klh} difficult and explains why these components are fault candidates.

5 Conclusions and Discussion

This paper describes the modeling process for a qualitative diagnosis model of a complex dynamic system. Qualitative modeling has the advantage that non linearities can be approximated and that parameter values do not have to be estimated. The model is successfully applied in a realistic setup. Results of an artificially introduced leak show that the FDI system TRANSCEND correctly hypothesizes the corresponding

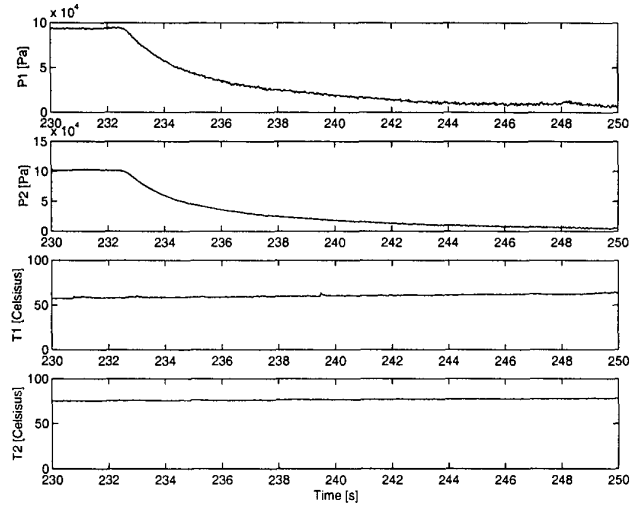

(a) Data segment

Step	T1	T2	P1	P2
0	(0, ·)	(0, ·)	(−, ·)	(−, ·)
1	(0, ·)	(0, ·)	(−,−)	(−,−)

(b) Signal to Symbol Transformation

step 1

		actual
	e61:	− −
	e46:	− −
	e5:	0 ·
	e4:	0 ·
$I_{rad}+$	e61:	− − +
	e46:	− − +
	e5:	0 0 −
	e4:	0 − ·
$C_{rair}+$	e61:	− − −
	e46:	− − −
	e5:	0 0 +
	e4:	0 0 −
$R_{rad}+$	e61:	− − −
	e46:	− − −
	e5:	0 0 0
	e4:	0 0 −
$R_{lkth}-$	e61:	− − +
	e46:	− − +
	e5:	0 0 −
	e4:	0 − ·

(c) Diagnosis result

Figure 6. FDI of leakage in the lower hose.

model parameter as a possible cause. Three additional parameters are hypothesized as fault candidates because the four measured variables do not provide sufficient discriminating information. Systematic measurement selection [13] will identify which additional variables need to be measured to further prune this set of four down to only the one actual deviating parameter and to achieve *complete diagnosability* in general.

In the experiment, the system was close to steady state and the thermostat was open. In general, during dynamic behavior the thermostat state may change between open and closed, causing a *structural change*. When the thermostat is open the radiator is a part of the coolant fluid whereas when it is closed only the primary circuit remains. In the present model, this phenomena has not been modeled. Modeling structural changes can be handled properly by the use of hybrid models [10] and their application to diagnosis will be explored in future research.

Acknowledgments

This research is supported by funds from Hewlett-Packard Laboratories, Palo Alto, California, USA. This work was carried out while Philippus Feenstra was a visiting scholar at Vanderbilt University in the Modeling and Analysis of Complex Systems Laboratory of the Department of Electrical Engineering and Computer Science.

References

[1] Electronics Development Corporation. *1451.2 OEM Embedded STIM kit - Technical Data Sheet*, 1999. http://www.smartsensor.com/data.htm.

[2] H. Engja. Bond graph model of a reciprocating compressor. *Journal of the Franklin Institute*, 319(1/2):115–124, January/February 1985.

[3] Hewlett-Packard Corporation. *BFOOT-66501 Embedded Ethernet Controller - Technical Data Sheet*, 1999. http://www.hpie.com/datasheets/bfoot66501/.

[4] IEEE. Standard for a smart transducer interface for sensors and actuators – transducer to microprocessor communication protocols and transducer electronic data sheets (TEDS) formats, IEEE std 1451.2, Sept. 26 1997.

[5] D. Karnopp, D. Margolis, and R. Rosenberg. *Systems Dynamics: A Unified Approach*. John Wiley and Sons, New York, second edition, 1990.

[6] K. Lee and R. Schneeman. Internet-based distributed measurement and control applications. *IEEE Instrumentation & Measurement magazine*, 2(2):23–27, June 1999.

[7] E.-J. Manders, G. Biswas, P. J. Mosterman, L. Barford, V. Ram, and J. Barnett. Signal interpretation for monitoring and diagnosis, a cooling system testbed. In *Proceedings of the IEEE Conference on Instrumentation and Measurement Technology (IMTC99)*, pages 498–503, Venice, Italy, 1999.

[8] E.-J. Manders, P. J. Mosterman, and G. Biswas. Signal to symbol transformation techniques for robust diagnosis in TRANSCEND. In *Tenth International Workshop on Principles of Diagnosis*, pages 155–165, Loch Awe, Scotland, 1999.

[9] P. J. Mosterman. *Hybrid Dynamic Systems: A hybrid bond graph modeling paradigm and its application in diagnosis.* PhD dissertation, Vanderbilt University, 1997.

[10] P. J. Mosterman and G. Biswas. Principles for modeling, verification, and simulation of hybrid dynamic systems. In *Fifth International Conference on Hybrid Systems*, pages 21–27, Notre Dame, Indiana, Sept. 1997.

[11] P. J. Mosterman and G. Biswas. Diagnosis of continuous valued systems in transient operating regions. *IEEE Trans. on Systems, Man and Cybernetics*, 29(6):554–565, 1999.

[12] P. J. Mosterman and G. Biswas. A java implementation of an environment for hybrid modeling and simulation of physical systems. In *ICBGM99*, pages 157–162, San Francisco, Jan. 1999.

[13] P. J. Mosterman, G. Biswas, and N. Sriram. Measurement selection and diagnosability of complex dynamic systems. In *Eighth International Workshop on Principles of Diagnosis*, pages 79–86, Mont. St. Michel, France, Oct. 1997.

[14] J. U. Thoma. Entropy and mass flow for energy conversion. *Journal of the Franklin Institute*, 299(2):89–96, 1975.